Bull. Spec. Astrophys. Obs., 1997, 43, 75–94

Precession and orbital variability of radial velocities in SS 433

S.N.Fabrika, L.V.Bychkova, A.A.Panferov

Special Astrophysical Observatory of the Russian AS, Nizhnij Arkhyz 357147, Russia

Received March 21, 1997; accepted May 20, 1997.

Abstract. A precession variability of emission line radial velocities in the spectrum of SS 433 and precession modulation of the orbital radial velocity curves have been found. The parameters of the orbital curves change considerably with precession phase. The phases are isolated when the line profiles are least distorted by the contribution of gaseous streams and the absorption in the wind from the accretion disk. On this basis a correct SS 433 mass function has been found, which shows that the system is massive and its relativistic component has a mass of $2.1 - 3.8\,M_\odot$. The emission lines radial velocities and intensities variation with precession phase is shown to be due to the absorption in the wind from the accretion disk. Even the line He II 4686 Å in the profile of which the absorption line is not clearly observed, is subject to this effect. The radial velocities of absorption lines are found to be strongly dependent on the precession phase, but no significant dependence of them on the orbital phase is shown to exist. The structure of gas outflow from the accretion disk is found. In the disk plane the dense gas outflows at a low velocity, 0 – 100 km/s, which is likely to occur mainly through the libration point L_2. When approaching the disk axis, the gas density decreases, while the observed wind velocity rises to 600 – 1200 km/s, depending on the line optical thickness. The gas optical thickness sufficient for a strong absorption line to be appeared is gained at a distance from the system of $4.5 \cdot 10^{13}$ cm. This effect causes the observed delay of about 20 days in the appearance of the absorption lines in the spectrum with respect to the "edge-on" disk position and the same delay of emission line radial velocity precession curves. A number of new periods in the emission line radial velocity variations have been found, many of which are multiple of the precession period. The period 23.228 ± 0.005 days, which corresponds to 1/7 of the precession period, is the most significant. It is shown that these periodicities can not be due to the variability of the absorption line components. The periods are likely to be evidence of spiral shock in the accretion disk of SS 433.

Key words: stars: close binary: individual (SS 433) – accretion disk – radial velocity

1. Introduction

The unique binary system SS 433 (= V1343 Aql) has been studied by many authors for the last 18 years. The spectrum of SS 433 is quite complex. Apart from the stationary emission lines of hydrogen, He I and He II the narrow absorption lines H I, He I and Fe II with the P Cyg type profiles are present in it. As a rule, the parameters of these emission lines change with a phase of the 13–day orbital period. Besides, in the spectrum are present moving hydrogen and He I emission lines which are formed in the relativistic jets of SS 433. The location of these lines in the spectrum depends on the phase of the 162–day period, the half-amplitude of their displacement amounts to 1000 Å.

To answer the questions concerning the evolutionary status of the object, the processes developing in the system, it is very important to study the spectral line radial velocities. The behaviour of the SS 433 spectral line radial velocities has been studied by Crampton et al. (1980), Crampton and Hutchings (1981). They were the first to derive the dependences of the radial velocities of the stationary emission lines Hβ and He I and the absorption lines He I and Fe II λ 5169 on the orbital phase. They have also revealed the intensities of these lines to vary with precession period phase and suspected precession modulation of the radial velocities of the hydrogen emission lines and He I. The absorption line radial velocities have been suspected to be determined by the intensity and the behaviour of the emission lines. The authors suppose that since the Fe II line has no emission component, it may be free of such a variability.

The variability of spectral lines of SS 433 with orbital period has been studied by Kopylov et al. (1989).

They presented detailed radial velocity curves of the main spectral lines and also of the high temperature emission line He II and the blend C III, N III $\lambda_{\rm eff}$ 4644. The authors pointed out that there is a relation between the radial velocities of the stationary emission lines Hβ, Hγ and He II and the precession period phase. They attempted to allow for the effect of precession with the aid of systematic radial velocity shifts obtained in different months of observations. However, this correction for the emission lines did not give significant results. Nevertheless, for the absorption lines of P Cyg type the correction allowed the authors to derive orbital radial velocity curves of the lines Hγ, Hα, He I λ 4471, He I λ 5876, Fe II λ 5169.

The radial velocity curves of the hydrogen and He I lines show that these lines are formed in the gaseous streams (Fabrika et al., 1997 a) and therefore can not be used for direct measurements of the masses of the components in the system SS 433. He II λ 4686 is the only line in the SS 433 spectrum which is formed mainly in the accretion disk or in the wind outflowing from the disk. The centre of gravity of this line reflects the relativistic companion motion. Earlier Fabrika and Bychkova (1990), when studying the He II line radial velocities, revealed the radial velocity curve to have two states, depending on the precession phase. For the phases $0.9 < \psi < 0.1$, when the disk faces the observer to a maximum, the disk emission is dominant in the line profile. The second state, for the adjacent precession phases, is characterized by predominance of radiation of the gaseous stream directed to the accretion disk (see also Fabrika et al. (1997 a, b).

Proceeding from the above data, at least two such states, as in the He II line, seem likely to be present in other spectral lines of SS 433 too. This assumption is also confirmed by a high scatter of the data in the orbital radial velocity curves, which is much higher than the measurement errors. All these suggest a considerable precession modulation of spectral lines of the system. That is why it is important to examine the precession radial velocity curves corrected for the orbital variability. The solution of this problem and the study of the behaviour of the orbital curves in different intervals of the precession period seem possible since we possess a considerable body of spectral data on SS 433 obtained at the Special Astrophysical Observatory. In this paper we use new data along with the data already published by Kopylov et al. (1989).

2. Observational data and analysis procedures

Spectroscopic observations of SS 433 were performed with the 1000-channel TV–scanner (IPCS) of the 6 m telescope of SAO. The procedure of observations with this device, the sequence and stages of digital processing of spectral data, the positional and photometric accuracy are described by Kopylov et al. (1985, 1986 a).

We used for the analysis the data for 11 nights of observations in 1980 (51 spectrum) and for 35 nights in 1981 (258 spectra) which have been already described by Kopylov et al. (1989). We have also used the data of 12 nights obtained in 1982 (38 spectra), 13 nights in 1986 (46 spectra), 11 nights in 1987 (17 spectra), 3 nights in 1988 (8 spectra), 14 nights in 1989 (38 spectra) and 4 nights in 1990 (19 spectra). All the spectra were taken using the same devices and the same grating. The spectral resolution was, on the average, about 4 Å. The spectral range of a single spectrum was about 1800 Å. From 1980 to 1982 the spectra were obtained, as a rule, from the blue to the red range (Kopylov et al., 1985; 1986 b; 1987; 1989). Since 1986 we have done spectroscopy of the object basically only in the blue region of the spectrum. At this time SS 433 has been observed mainly within the co–operative programmes in the orbital phases close to the primary minimum with the aim of defining the structure of the accretion disk. More detailed information about the spectra obtained in the frames of the co–operative programmes can be found in Fabrika et al. (1997 b).

We have studied the stationary emission lines Hβ, He II λ 4686, He I λ 5876, He I λ 6678, He I λ 7065 and the P Cyg type absorption line components — Hβ, He I λ 4922, He I λ 5015 of (the latter two are blended by the weak lines of Fe II) and Fe II λ 5169. The He I lines located in the red part of the spectrum have very weak absorption components which are not always conspicuous. On the other hand, since the object is bright in the red region the emission line profiles of these lines could be measured with a good accuracy. The lines that were blended by the moving emission lines of the jets as well as weak or noisy lines were not measured. The Hβ line in the spectrum of SS 433 is very intensive, that is why we have measured the radial velocities of this line both from the peak (p) and from the centre of gravity (c. g.). For the other lines we used the radial velocity measurements from the profile centre of gravity alone. The He II line radial velocities had to be given a specially careful study since it is the only line that reflects the orbital motion of the relativistic star and can be used for measuring the masses of the components. For analysis of this line, only relatively symmetric profiles unblended by the moving lines and undistorted by the strong blend C III, N III $\lambda_{\rm eff}$ 4644 were used. The He II line radial velocity measurements were made from the centre of gravity not from the whole line, but only from the central regular and structureless part of it. Only the wings of the line were cut off since the noises and the complexity of the profile in the wings may introduce a considerable error in measurements us-

ing this method. In the processing we used the programmes of reduction of spectra described by Kopylov et al. (1986 b) and also the programme SPE created by S.S. Sergeev at the Crimean Astrophysical Observatory.

The moment of the primary minimum Min I was adopted as a zero phase of the orbital period, when the optical star eclipses the accretion disk. The orbital phases are calculated as (Fabrika et al., 1990)):

$$\text{Min I} = \text{JD } 2445942.204 + 13.0815 \cdot \text{E}.$$

The moment T_3, when the disk faces the observer to a maximum (the maximal spread of the moving lines over the spectrum), is taken as a zero precession phase (Margon and Anderson, 1989):

$$T_3 = \text{JD } 2443506.78 + 162.50 \cdot \text{E}.$$

Our data cover well the orbital phases. They cover the precession phases between 0.6 and 0.2 in the same way, however, we have almost no observations at the rest of the precession phases.

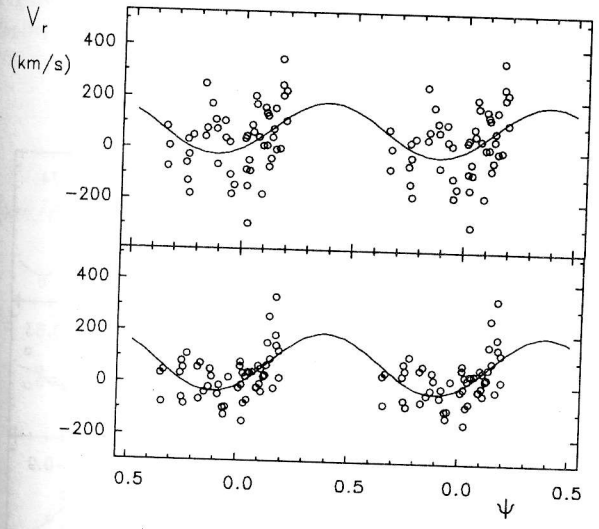

Figure 1: **a.** *The He II λ4686 emission line radial velocities versus precession phase: top — the original data, bottom — the data corrected for the orbital variability.*

Figs. 1a–6a present the relationships between the radial velocities of the emission lines He II λ 4686, Hβ (p), Hβ (c. g.), He I λ 5876, He I λ 6678, He I λ 7065 and the precession phase. When studying the radial velocities of the Hβ line peak it appeared possible to add the radial velocities taken from Crampton et al. (1980); in Fig. 2a the data added together are presented. In the cases when we had more than one spectrum a night the average line radial velocities were used. The radial velocity measurement error depends on the spectrum quality and on the line intensity and makes on the average (rms) 25–30 km/s in our measurements. The scatter on the presented curves is considerably larger, which is due to the orbital variability and also to the sporadic activity of the object itself. Viewing Figs. 1a–6a, several conclusions can be drawn:

- there are considerable, sinusoidal in a first approximation, variations of emission line radial velocities with precession period phase,
- the half-amplitude of these variations is 100–140 km/s,
- the phase of the radial velocity maximum is about 0.7 with the exception of the line He II (about 0.4), for which our data cover insufficiantly the precession period,
- the scatter of points for the curves is considerable, especially near phases 0.1 and 0.7.

Since the scatter is mainly associated with the orbital variability, it was decided to analyse the orbital curves in the narrow intervals of the precession phases to separate the precession and orbital variabilities.

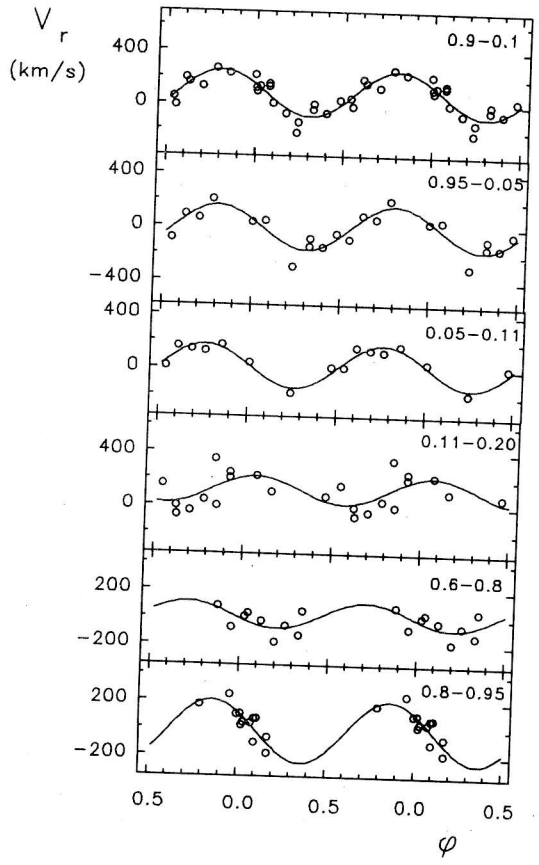

Figure 1: **b.** *The He II λ4686 emission line radial velocities versus orbital phase in the precession phase intervals (shown in the figure) used for the correction. The curve in the interval of ψ 0.9–0.1, from which the mass function has been obtained, is also shown.*

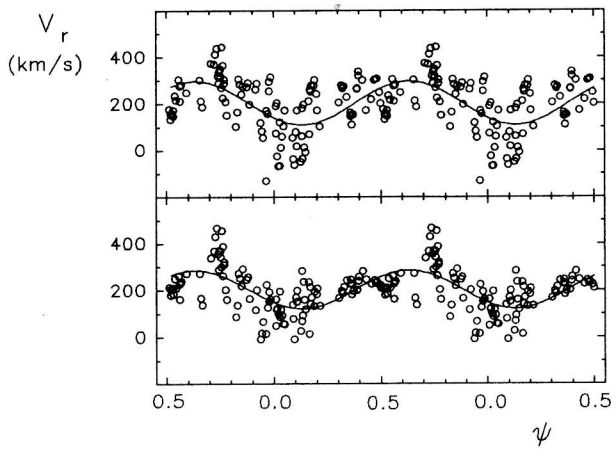

Figure 2: **a.** *The* Hβ *(p) emission line radial velocities (the same as in Fig. 1 a).*

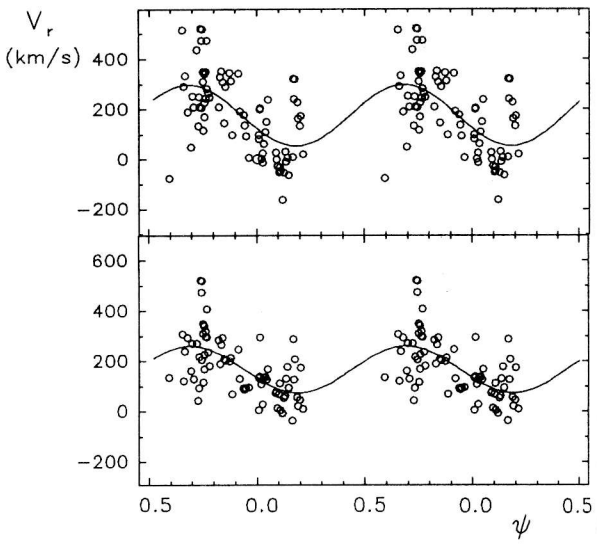

Figure 3: **a.** *The* Hβ *(c. g.) emission line radial velocities (the same as in Fig. 1 a).*

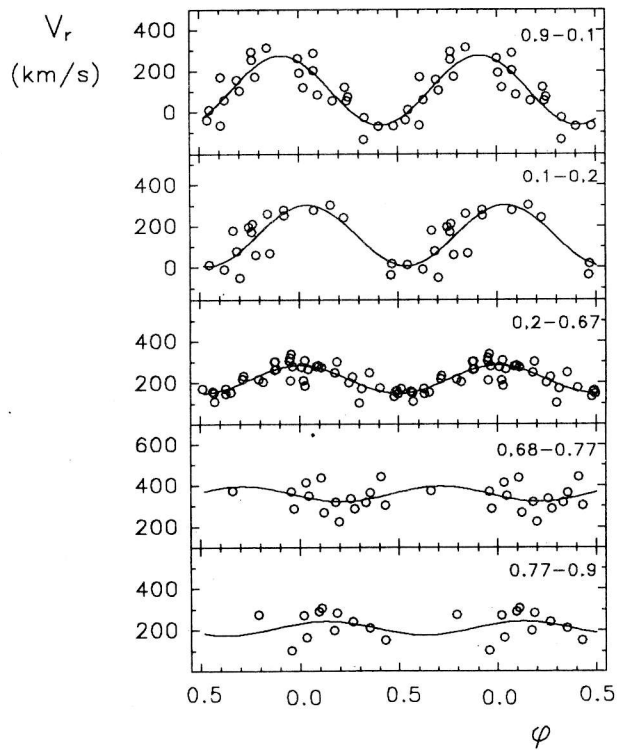

Figure 2: **b.** *The* Hβ *(p) emission line radial velocities (the same as in Fig. 1 b).*

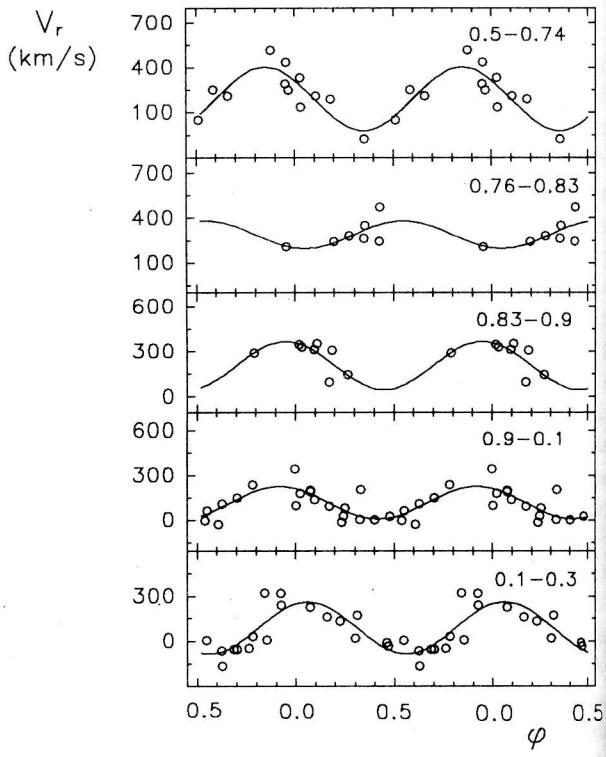

Figure 3: **b.** *The* Hβ *(s. g.) emission line radial velocities (the same as in Fig. 1 b).*

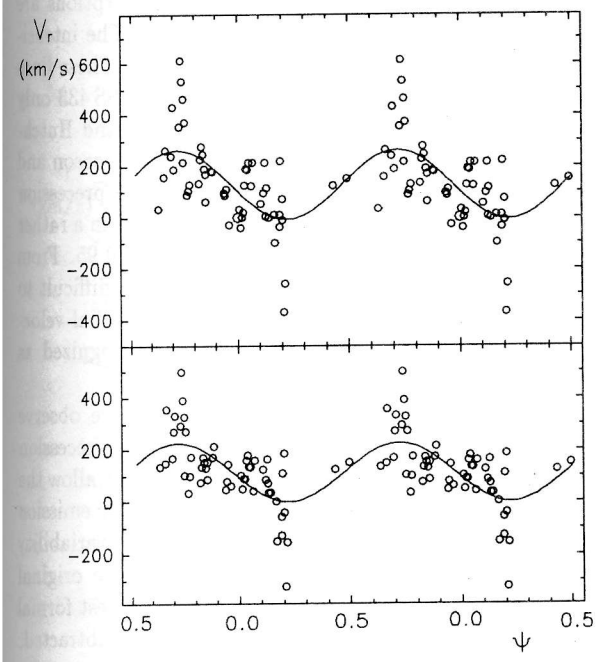

Figure 4: **a.** *The He I λ5876 emission line radial velocities (the same as in Fig. 1 a).*

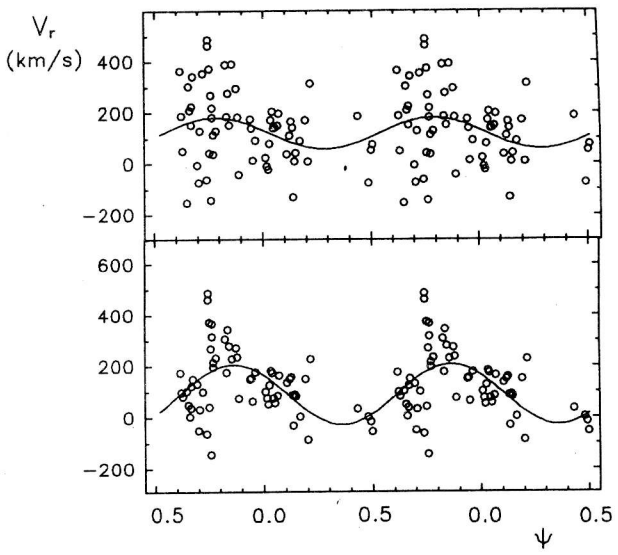

Figure 5: **a.** *The He I λ6678 emission line radial velocities (the same as in Fig. 1 a).*

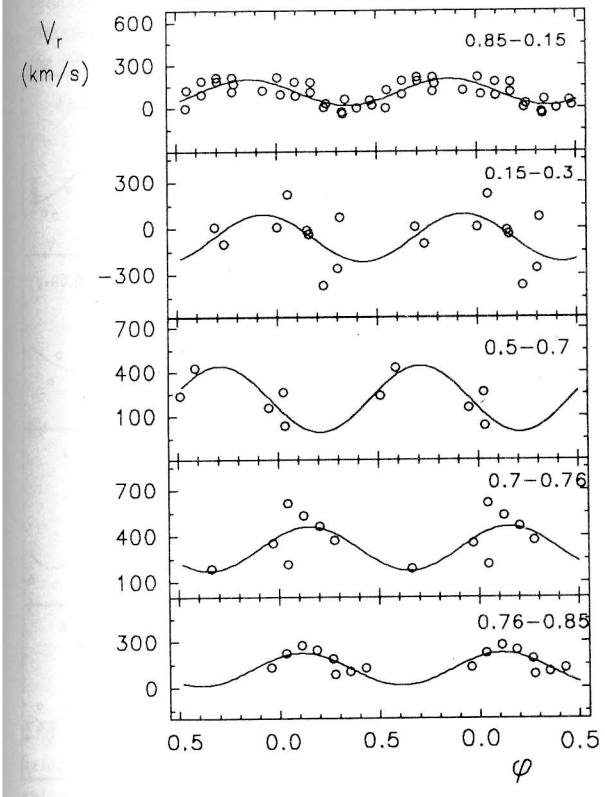

Figure 4: **b.** *The He I λ5876 emission line radial velocities (the same as in Fig. 1 b).*

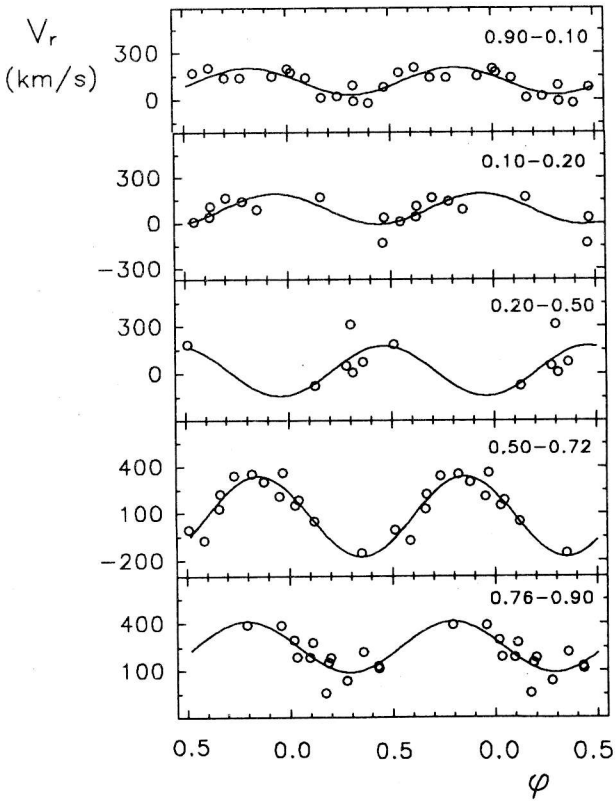

Figure 5: **b.** *The He I λ6678 emission line radial velocities (the same as in Fig. 1 b).*

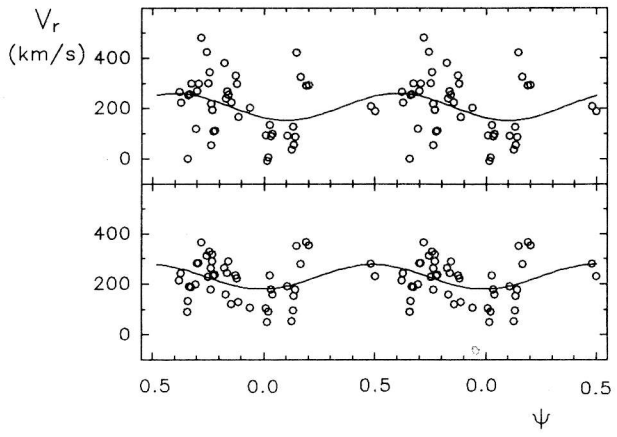

Figure 6: **a.** *The He I λ7065 emission line radial velocities (the same as in Fig. 1 a).*

Figs. 1 b – 6 b present the orbital curves which were used to allow for the orbital variability in the precession radial velocity curve. The orbital curves were fitted with sine function with the three free parameters: the γ–velocity V_0 (the mean velocity of the curve), amplitude K and the zero phase ϕ_0. The orbital curves we obtained for different phase intervals of the precession period $\Delta\psi$. The boundaries of these intervals were varied until the following conditions were fulfilled: sufficient number of points to construct the orbital curve in a narrow interval $\Delta\psi$, sufficiently good covering of the orbital phases, minimum scatter of points for the curve. These conditions were not always possible to fulfil. It was especially difficult to find a regular orbital curve in the precession phase interval 0.7 – 0.9, which is likely to be due to real processes in the system SS 433 that lead to the variability of the observed radial velocities. In uncertain cases and in cases when the number of points in the interval $\Delta\psi$ was insufficient for the curve to be constructed, the approximation was not performed, and for further analysis the mean velocity in this precession interval was used.

In each selected precession phase interval the best orbital curve in the form $V_0 + K \cdot \cos(\phi - \phi_0)$ was found. Then in each the interval the variable part $K \cdot \cos(\phi - \phi_0)$ was subtracted from the data. The cleaned from the orbital variability radial velocities obtained in this way are presented as a function of precession phases in Figs. 1 a – 6 a at the bottom. As is seen from the figures, after the correction for the orbital variability the scatter of points on the precession curves became considerably smaller.

Figs. 7 – 10 show radial velocities of the absorption P Cyg type line components for Hβ, He I + Fe II λ 4922.9, He I + Fe II λ 5017.0 and Fe II λ 5169. The presentation is the same as for emission lines in previous fugures. In contrast to the emission lines the radial velocities of the absorptions are strongly variable with precession phase. The intensity of these lines is also strongly variable. These lines are known to appear in the spectrum of SS 433 only at precession phases 0.3 – 0.9 (Crampton and Hutchings, 1981; Kopylov et al., 1989). For this reason and because of the not complete covering the precession phases in our data, the radial velocities are in a rather narrow precession phase interval, 0.65 – 0.95. From the data presented in Figs. 7 a – 10 a it is difficult to draw a conclusion about the precession radial velocity curve. The obtained relations are recognized as fragments of large amplitude curves.

The narrow phase interval in which we observe the absorption lines as well as the strong precession variability of their radial velocities does not allow the technique described above to be used for the emission lines. For the absorption lines the orbital variability was found in the following manner. In the original radial velocities (Figs. 7 a – 10 a, top) the best formal curve as a sine function was found and subtracted. Thus we got rid of large amplitude precession variations and had an opportunity to analyse the weak orbital ones. After that, in a manner similar to that with the emission lines the orbital radial velocity curves (Figs. 7 b – 10 b) in the selected precession phase intervals were analysed and subtracted from the origi-

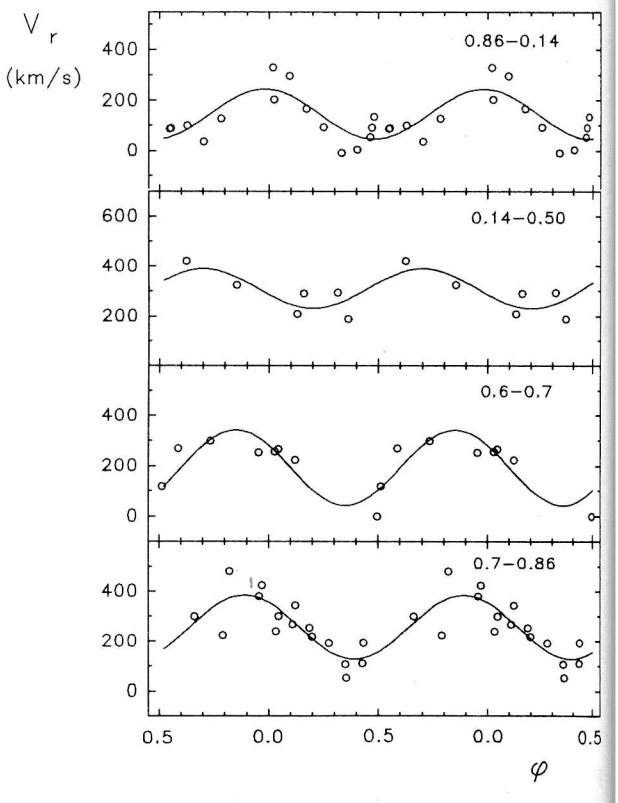

Figure 6: **b.** *The He I λ7065 emission line radial velocities (the same as in Fig. 1 b).*

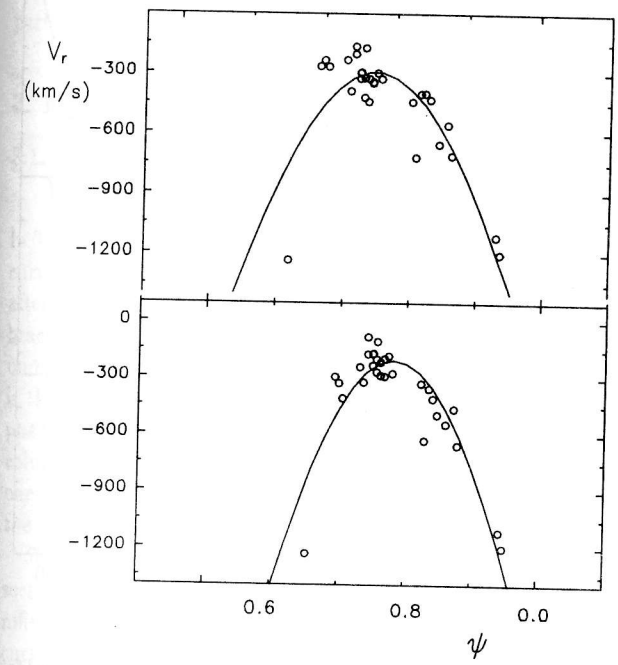

Figure 7: **a.** *The* Hβ *absorption line component radial velocities (its formal approximation is shown) versus precession phase: top — the original data, bottom — the data corrected for possible orbital variability.*

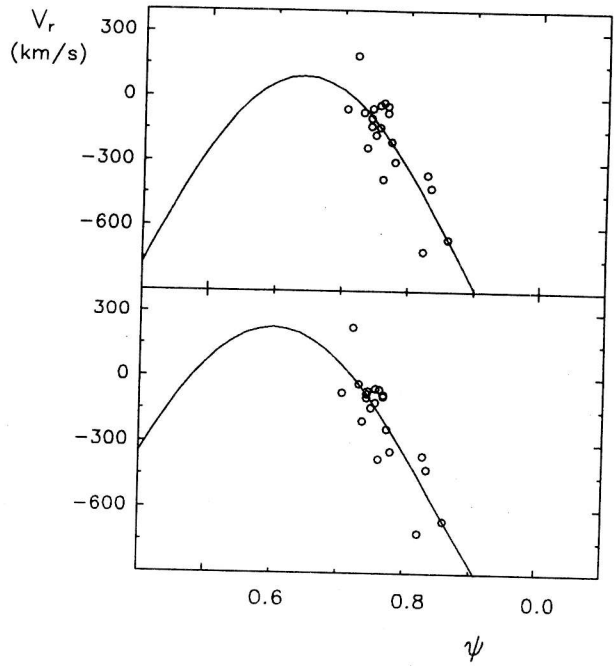

Figure 8: **a.** *The absorption line component radial velocities of the blend He I + Fe II* λ4922.9 *(the same as in Fig. 7 a).*

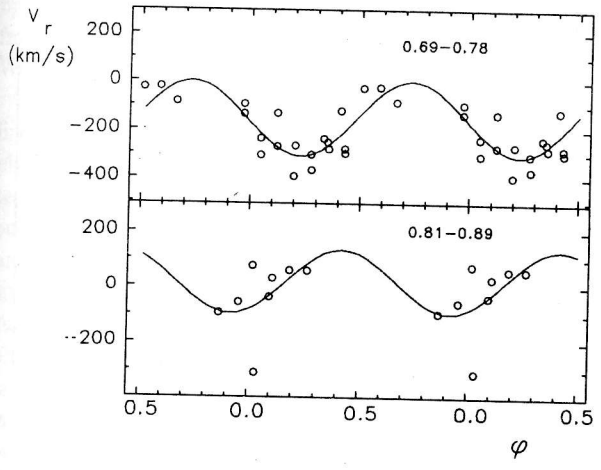

Figure 7: **b.** *The* Hβ *absorption line component radial velocities versus orbital phase in the precession phase intervals (shown in the figure) used for the correction. The radial velocities zero is formal coming from the precession curve fitting in Fig. 7 a.*

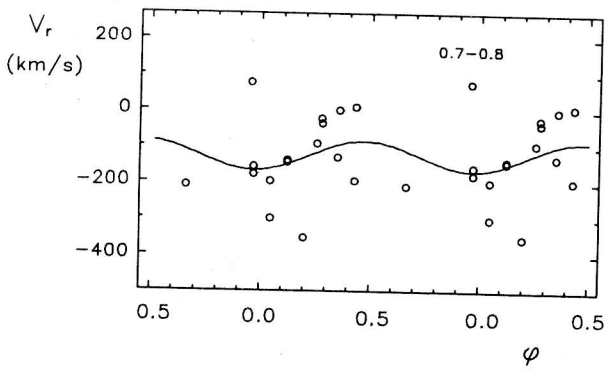

Figure 8: **b.** *The absorption line component radial velocities of the blend He I + Fe II* λ4922.9 *(the same as in Fig. 7 b).*

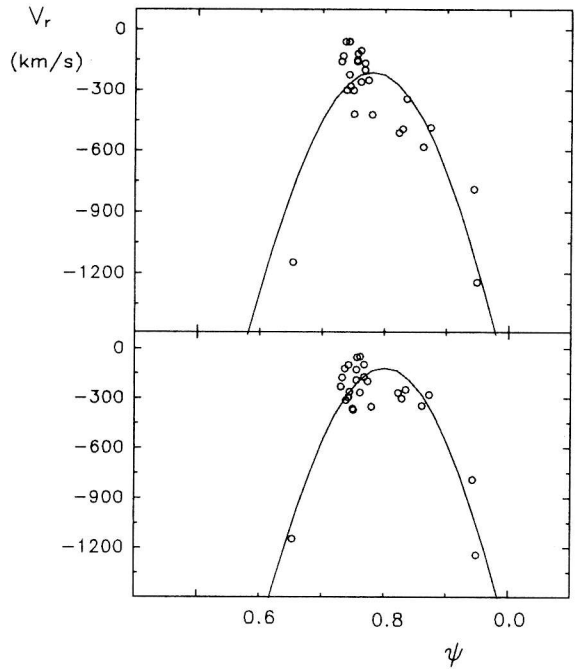

Figure 9: **a.** *The absorption line component radial velocities of the blend He I + Fe II λ5017.0 (the same as in Fig. 7 a).*

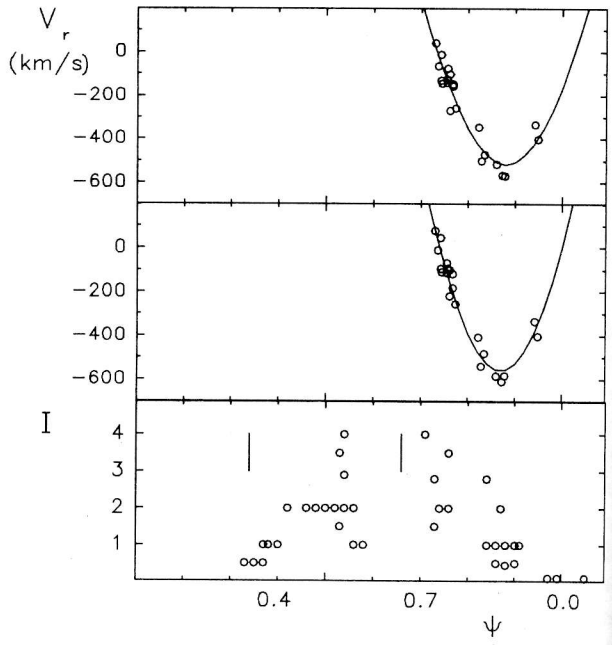

Figure 10: **a.** *The absorption line component radial velocities of the He II λ5169 (the same as in Fig. 7 a). In the bottom absorption line intensities of He I and Fe II are shown from the data of Crampton and Hutchings (1981). The vertical bars mark the "edge on" positions of the accretion disk.*

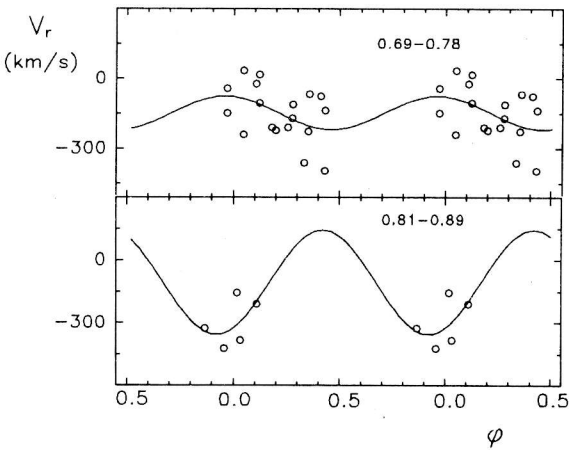

Figure 9: **b.** *The absorption line component radial velocities of the blend He I + Fe II λ5017.0 (the same as in Fig. 7 b).*

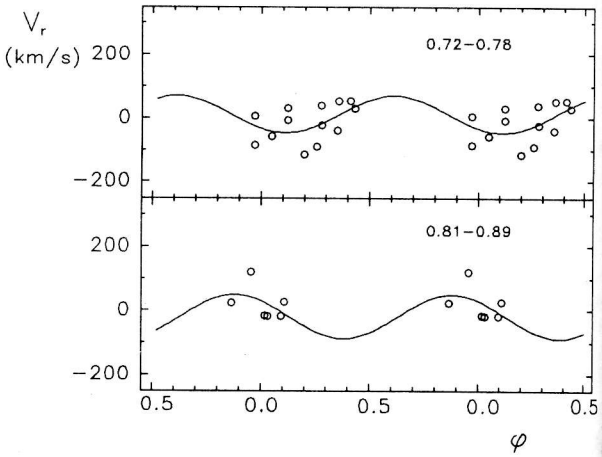

Figure 10: **b.** *The absorption line component radial velocities of the Fe II λ5169 (the same as in Fig. 7 b).*

nal data. The orbital radial velocities zero point is a formal coming from the formal precession curve fitting. The final precession radial velocity curve cleaned from the orbital modulation is displayed in the lower part of Figs. 7 a – 10 a.

3. Results

3.1. The precession modulation of the radial velocities

In Table 1 are listed the parameters of the precession curves of the emission line radial velocities before and after allowance for the orbital modulation (values in brackets). In the first column are indicated the lines under study; the second is the γ–velocity V_0; the third is the half–amplitude K; the forth column gives the phase ψ_m of the radial velocity maximum; the fifth column represents the scatter of data — the rms of one point; the number of points N used for deriving the curves is given in the last column.

From the data of Table 1 and Figs. 1 a – 6 a it is seen that consideration of the orbital modulation significantly reduces the scatter of data in precession curves. It can be said that in the cases when the precession modulation was pronounced from the original data and had a large amplitude K (lines Hβ, He II, He I λ5876) the correction for the orbital variability actually did not affect the precession curve shape, but decrease considerably the scatter of points. The precession curves in two red He I lines suffered a stronger change, their signal–to–noise ratio also increased. Of all these lines the He II is more pronounced, its precesion curve leads the rest of the lines, on the average, by a phase interval of 0.3. This line is distinguished from the rest of the lines by a number of properties. We will discuss this below.

Except for the Hβ (p) line, the data for the other lines do not cover completely the precession period in phases. For this reason we believe that the parameters of the precession curve have been found reliably only for this line. The reduction of the data scatter around the precession curves is not by itself a conclusive reason for reality of the radial velocity precession curves. In Fig. 11 are shown the γ–velocity V_0 and the phase ψ_m of the curves maximum versus their half–amplitude K for the lines from Table 1. The circles indicate the values of the parameters before the orbital variability was allowed for, the triangles indicate the values after the subtraction of this variability (Table 1, the values in brackets). If the parameters of the curves derived from the original data in no correlate with one another, after taking into account the orbital modulation these parameters are distinctly seen to depend on each other. The appearance of these relations after the orbital variability subtraction is a direct indication of reality of the emission line radial velocity precession curves. The He II line shows a minimal γ–velocity and accordingly a maximal half–amplitude. The phase of the precession curve maximum of this line does not fall in any way within the generality. In this figure are exhibited the best approximations of the data obtained from the curves corrected for the orbital modulation (the second relation is derived without He II):

$$V_0 = 136 + 3.6 \cdot K - 0.035 \cdot K^2,$$

$$\psi_m = 0.38 + 0.0014 \cdot K + 0.00002 \cdot K^2.$$

The relationship found — decrease in half–amplitude of the precession curves with increasing γ–velocity — can be understood. The emission lines undergo absorption in the blue wing of their profiles. The more the line profile is distorted by absorption the larger the shift of the emission line centre of gravity towards the red wavelengths and the smaller the amplitude of radial velocity variations. This is possible in the case if the regions of emission and absorption are isolated. The resulting displacement of an emission line is determined by a relative contribution of absorption to the total profile and by the absorption line position in the blue part of the profile. We see that all emission lines in the spectrum of SS 433 are distorted by absorption. Even the He II line is subject, but in the least degree, to this effect. The true radial velocity of SS 433 is close to zero (Crampton and Hutchings, 1981; Fabrika and Bychkova, 1990), only the He II λ4686 line centre of gravity has such a velocity at precession phases $\psi \approx 0$.

The line He II falls out sharply of the relation ψ_m — K. This is probably due to the fact that, in contrast to other lines, an important role in the formation of He II is played by the region in accretion disk around the jets bases. As it has been found (Fabrika and Bychkova, 1990; Goranskij et al., 1997; Fabrika et al., 1997 a), this line consists of two principal components that are formed: 1) in the central parts of the accretion disk (the broad component, eclipsed at the orbital phase $\phi = 0$) and 2) in the gas stream directed to the disk (the bright narrow component, eclipsed at $\phi = 0.1$). In the region of the precession phase $\psi = 0$, when the accretion disk is exposed to the observer, the relative contribution of the second component markedly decreases, and the radial velocity of the total He II profile approaches zero. At the adjacent phases (when the line of sight is closer to the disk plane) the contribution of the streams grows, the γ–velocity rises to 100 km/s. In Fig. 1 b one can see the changes in the radial velocities of the orbital curves of this line in different precession phases. Goranskij et al. (1997) and Fabrika et al. (1997 a) have shown that, as distinct from He II, the Hβ line is formed completely in the stream (or the stream component is dominant at all precession phases). From all this it

Table 1: *Parameters of the emission line precession radial velocity curves*

Line	V_0 km/s		K km/s		ψ_m		rms km/s		N
He II λ4686	80	(81)	103	(114)	0.38	(0.39)	120	(76)	52
Hβ (p)	204	(204)	93	(81)	0.63	(0.63)	97	(74)	110
Hβ (c. g.)	176	(169)	121	(93)	0.68	(0.79)	123	(93)	75
He I λ5876	128	(113)	135	(112)	0.72	(0.72)	130	(104)	55
He I λ6678	120	(90)	61	(117)	0.78	(0.86)	140	(111)	62
He I λ7065	207	(229)	53	(48)	0.60	(0.49)	111	(79)	45

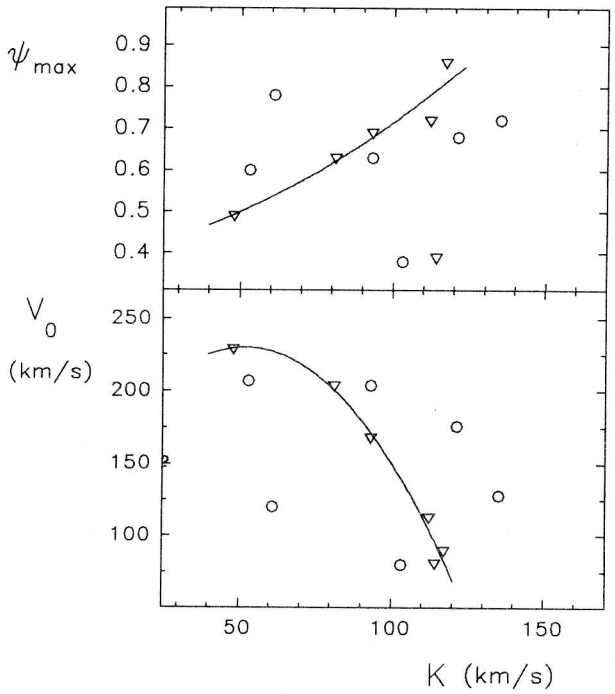

Figure 11: *Relations between the parameters of the emission lines precession radial velocity curves (from Table 1). The circles indicate the parameters before the orbital variability was allowed for, the triangles indicate the values after the subtraction of this variability.*

can be concluded that the causes of precession variability may be different in the Hβ and He II lines. In particular, in the He II line in the vicinity of $\psi = 0$, the region around the approaching jet is best seen, the opposite region is obscured by the disk. In the vicinity of $\psi = 0.5$ the reverse is true. In this case a precession variability in the He II may be expected of approximately the same type seen in Fig. 1 a.

The relations presented in Fig. 11 suggest that the effects of absorption play a vital role in forming the line profiles. The intensification of the absorption lines displaces the emission line centre of gravity redward. From this follows a natural interpretation of the radial velocity precession curves themselves. In the vicinity of precession phases 0.3 – 0.7, when the disk is basically viewed edge–on, the absorption in the blue wing is enhanced, and the line centre of gravity is displaced redward. At precession phases near zero the absorption weakens, the distortion of the lines becomes less, their centres of gravity shift blueward, closer to their normal position. The absorption lines originate in the wind outflowing from the system. The density and velocity of gas in the wind depend on the orientation of the accretion disk, therefore the disk is the wind source. We will see below that the behaviour of the absorption lines confirms this idea. In this interpretation the maximum on the radial velocity curves must be located at precession phase 0.5. In fact, we observe a delay of the curves by $\Delta\psi$ (em) $\approx 0.12 \pm 0.07$ on the average over all lines of Table 1. The Hβ (p) line, for which the most reliable precession curve is available, yields the delay $\Delta\psi$(Hβ) = 0.13 or 21 days. Different lines, nevertheless, show different delays of the radial velocity maximum with respect to precession phase 0.5, and this manifests itself in the relation between ψ_m and the half–amplitude K.

3.2. Analysis of new periods

In first approximation the precession curves are actually sinusoidal. However, they show well the effects which manifested themselves just after the orbital variability was taken into account. These are modulations of the radial velocitues with a total amplitude between 100 and 500 km/s. These new types of variability themselves are also nearly sinusoidal and different at different precession phases (Figs. 1 a – 6 a, bottom). They are also different for different lines. The precession period modulations are best seen in the radial velocities measured from the Hβ (p) line (Fig. 2 a). Here we have the largest body of data, the line is the strongest in the blue region of the SS 433 spectrum and its measurement accuracy is higher than in other lines. From Fig. 2 a the modulation can be concluded to be complex and consisting of, at least, two different periods. The periodicity of about 40 – 60 days (or $\delta\psi = 0.2 - 0.4$) is pronounced at $\psi = 0.3 - 0.6$

and also becomes noticeable at $\psi = 0.9 - 0.2$. The period of about 20 days (or $\delta\psi \approx 0.15$) shows up at phase 0.7, where its amplitude is very large, and is traced down to 0.0. It is seen well that the character of these periodicities differs dramatically at different precession phases, i. e. it depends on the angle at which the accretion disk is observed.

To analyse the radial velocity modulations, we have chosen the line Hβ(p) and divided the whole collection of data into three intervals in precession phases ψ: 1) 0.25–0.6, 2) 0.6–1.0 and 3) 0.9–1.25. Examining Fig. 2 a, it may be assumed that different types of variability are peculiar to each of these intervals. In the first interval a period of 50 days is well seen, the half–amplitude of the velocity variation with such a period is about 100 km/s. This principal modulation is distorted by a shorter period or a few periods. It is important that all radial velocities of this interval are taken from Crampton et al. (1980) obtained from a continuous series of observations during a single precession cycle. This means that the accuracy of the search for periods in this interval can not be high because of the short observing row. In the second interval a very strong modulation with a period of about 20 days is apparent. The half–amplitude of the radial velocity variations with this period ranges from 200 km/s at phase 0.7 to about 100 km/s at 1.0. The third interval is more complex, nevertheless, the radial velocity curve is readily seen to be stratified into several harmonics with approximately equal amplitudes. It may well be that the large period ($\approx 40 - 60$ days) observed in the first interval appears here again.

In order to analyse the periodicities, the precession modulation shown in Fig. 2 by the solid line was subtracted from the data. Thus, the radial velocities, from which both the orbital and the precession variabilities had been subtracted, were analysed. The time interval in which the data are distributed is about 11 years. The search for periods in the radial velocities, as dependent on Julian Date, was made by means the data approximation by the sinusoid using the least-squares method. It is of vital importance to note that since some periodicities are directly seen on the precession phase diagram (the lower plot in Fig. 2 a), they are, firstly, real and, secondly, multiple of the precession period, $P_{pr} = 162.5$ days. This point has to be taken into account first of all when interpreting the new periodicities of the SS 433 radial velocities.

In Table 2 we present the precession phase intervals, the number of radial velocity measurements n of the Hβ(p) line in each interval, the periods found and the mean root–mean–square deviations from the best curve $<$ rms $>=$ rms$/\sqrt{n}$. The table gives only the most prominent periods of the most power. The periods multiple of the precession one are indicated in the notes. Since the data were taken in the precession phase intervals, occurrence of beatings with the period P_{pr} as well as typical for such cases annual harmonics (labeled by $\pm$ y in Table 2) should be expected. If the periods multiple of P_{pr} are available and real in the data, their beatings with P_{pr} will cause the appearance of new harmonics which will also be multiple of P_{pr}. The latter harmonics must not appear when analysing all the data without selection in phase intervals. Nevertheless, from the right part of Table 2 it follows that in this case multiple periods 1/3, 1/4, 1/6, 1/7, 1/9 are revealed. It is not improbable that some of them are still the result of beatings, i. e. our approximation of the precession variability (by the sine function) may be not fair enough. In consequence of this, in the corrected radial velocities there may remain a variability with the period P_{pr}, which means that additional multiple harmonics may appear.

The presence in a main period (or several periods) of precession or annual harmonics suggests that the period is real, i. e. it is related to a certain physical process. A more detailed study, including the analysis of low–power harmonics (from the data not only in the Hβ line but also in other lines) will be published elsewere. Here we pay an attention only to the periods that are "seen by eye" in Fig. 2 a and, therefore, certainly real. This is a 60–days period in the precession phase interval $\psi = 0.3 - 0.6$ and the period of 23.228 days at $\psi = 0.6 - 1.0$. Regarding the first period, we can only register the fact of its presence and can not measure it precisely, because all the observations in the interval No. 1 were performed within a single precession cycle, whereas in the interval No. 2 we can measure the second period with a fair accuracy (see also Fig. 13 below). It is estimated as 23.228 ± 0.005 days where the error is 1 standard deviation. Under the assumption that this period is a 1/7 of the precession period, we derive a value of 162.60 ± 0.04 days for the precession period. The accuracy of precession period determination by this procedure is no worse than in estimating it directly from the relativistic lines of the jets. The obtained value is in good agreement with the precession period (Margon and Anderson, 1989) estimated in a simple 5–parameter model (162.50 ± 0.03), in a 6–parameter model with a variable period (162.71 ± 0.11) and in a simple sinusoidal model (162.54 ± 0.03).

As to reality of the rest of the multiple periods from Table 2, we are not certain. It is not improbable that the period of 20.31 days (1/8) in the interval No. 2 is a harmonic of the period 1/7, while in the interval No. 3 the periods of 23.28 days (1/7) and 17.91 days (1/9) are harmonics of the periods 1/6 and 1/10, respectively. In this case it turns out that the radial velocities of the second precession interval are modulated only by the odd multiple periods (1/3, 1/7),

Table 2: *The periods of the* Hβ *(p) line radial velocities variability*

ψ (n)	Period (days)	<rms> (km/s)	Notes	ψ n	Period (days)	<rms> (km/s)	Notes
$\mathcal{N}1$	≈ 62	3.9			56.948	6.2	
0.25 – 0.6	≈ 22	6.6	$\approx 1/7$	0.0 – 1.0	54.408	6.0	$\approx 1/3$
(36)				(110)	52.139	6.3	
					41.002	6.0	$\approx 1/4$
$\mathcal{N}2$	62.189	9.4			38.501	6.2	
0.6 – 1.0	54.423	10.0	$\approx 1/3$		33.918	6.5	
(40)	45.016	10.6			26.985	6.4	1/6
	29.199	10.2	1/6 (–y)		24.107	6.6	
	23.228	9.6	1/7		23.225	6.4	1/7
	20.313	10.4	1/8		19.693	6.5	
	16.765	10.9			18.815	6.5	1/9 (–y)
					17.912	6.2	1/9
$\mathcal{N}3$	41.044	9.4	$\approx 1/4$		17.401	6.5	
0.9 – 1.25	30.434	9.1			17.188	6.4	1/9 (+y)
(45)	29.038	9.4	1/6 (–y)		15.455	6.6	
	26.942	9.8	1/6				
	23.701	9.5					
	23.279	9.6	1/7				
	18.825	9.5	1/9 (–y)				
	18.258	9.3					
	17.912	9.3	1/9				
	17.066	8.7	1/9 (+y), 1/10 (–y)				
	16.411	8.3	1/10				

while in the third interval they are modulated only by the even periods (1/4, 1/6, 1/10). At the given level of the analysis we can only state the fact of presence in the variability of the Hβ line radial velocities of periods multiple of the precession one. The precession period of SS 433 itself is not stable (Margon and Anderson, 1989). For this reason the accuracy of the new periods fit with the multiple periods (mainly inside $\pm 0.1 \div 0.2$ day) is quite good. The probability of random coincidence of the periods found with the periods multiple of 162.5 days is very low.

3.3. The precession modulation of the orbital variability. The mass function of SS 433

The radial velocity orbital curves derived at the narrow precession phases are presented in Figs. 1 b – 6 b. The precession modulation of the orbital curves was first suspected by Crampton and Hutchings (1981), Kopylov et al. (1989) and found in the line He II λ 4686 by Fabrika and Bychkova (1990). Here we present the data that show this modulation. The variability of the radial velocity orbital curves with precession phase of the accretion disk bears information on the structure of the disk itself and the gas streams in the system SS 433.

Our observations do not cover all precession phases for different lines so as to find reliably the orbital curves. Nevertheless, the basic regularities of the precession modulation can be readily seen in the figures. Table 3 presents for all the studied lines: the interval of precession phases, the γ–velocity of the orbital curve, its half–amplitude, the phase of intersection of the line radial velocity curve with its γ–velocity from the positive to the negative region (ϕ_{+-}), the rms of the best orbital curve and the number of points in the given interval of precession phases. In the cases when it was impossible to derive the orbital curve in the interval ψ, the table gives only the mean radial velocity V_0. The physical sense of the quantity ϕ_{+-}, i. e. the superior conjunction phase is a position of the centre of gravity of the emission line formation region and its azimuthal angle in the orbital plane of the system. The principal effect found is displacement of the phases of the orbital curves depending on the precession phase. The most "correct" orbital curves, i. e. the ones that represent the orbital motion of the components (or, in other words, the ones having the centre of gravity in the accretion disk or close to it), are obtained in the region of precession phase 0, when the disk exposes to the observer to a maximum. Here the orbital curve γ–velocity decreases (approaches the real radial velocity of SS 433), the half–amplitude grows. At other precession phases one

may observe considerable variations of ϕ_{+-}. The interpretation of this phenomenon is relatively simple and similar to that of the behaviour of the radial velocity precession curves. When the line of sight approaches the disk plane (precession phases different from 0) the contribution of the streams to the line profile grows and the self-absorption in the blue wing enhances, which leads to a decrease in half–amplitude and rise in gamma velocity. The He II line is mainly formed in the accretion disk region ($\phi_{+-} \approx 0$), but the Hβ line — in the stream ($\phi_{+-} \approx 0.25$), the He I lines take an intermediate position between He II and hydrogen. This follows from the orbital curves in the vicinity of $\psi \approx 0$, when the relative contribution of the stream is minimal. Since the stream contribution to formation of the He II line is the smallest of the rest of the lines, the phase of its orbital curve is the most stable (Fig. 2 b) and does not change dramatically at different precession phases.

The gas stream located close to the accretion disk may basically represent two active regions: the stream directed to the accretion disk and gas outflowing through the L_2 point on the opposite side from the disk. The location of the first region is directly seen (Figs. 1 b – 6 b, Table 3). These are phases $\phi = 0.1 - 0.25$, the values of ϕ_{+-} observed on the He I and Hβ curves. This is apparent even from the He II line at precession phases near 0.2 and 0.8. The stream in the vicinity of L_2 is not pronounced. To define the location of the emitting gas in this region may become possible through a modelling of the streams structure in SS 433 and comparing with the observational data obtained. In Fig. 12 we present the parameters of the Hβ (p) line orbital curve versus the precession phase. The effects described above are well seen in the figure. In particular, when the disk approaches to be viewed face-on ($\psi \approx 0$), the γ–velocity drops and the half–amplitude of the radial velocity curves grows. Strong absorption line appears in the Hβ profile at $\psi \approx 0.7$ (see below). At this moment the mean velocity rises sharply. Further up to phase 0 the absorption line intensity gradually decreases and the absorption itself is shifted blueward. The distortion of the emission line profile is diminished too, and the line is correspondingly shifted blueward. At this phase, 0.7, ϕ_{+-} suddenly drops and then increases. This may be related to both the distortion of the total Hβ profile by the absorption line and the manifestation of gas radiation at the point L_2. At this precession phase the disk is observed "edge-on". It is possible that it is at this phase that the contribution of the stream at the point L_2 grows since the emission line centre of gravity is displaced in the opposite direction ($\phi_{+-} = 0.96$) with respect to the accretion disk.

Analysis of the precession modulation of the He II line radial velocity curves will allow the problem of the SS 433 mass function to be solved. The profile

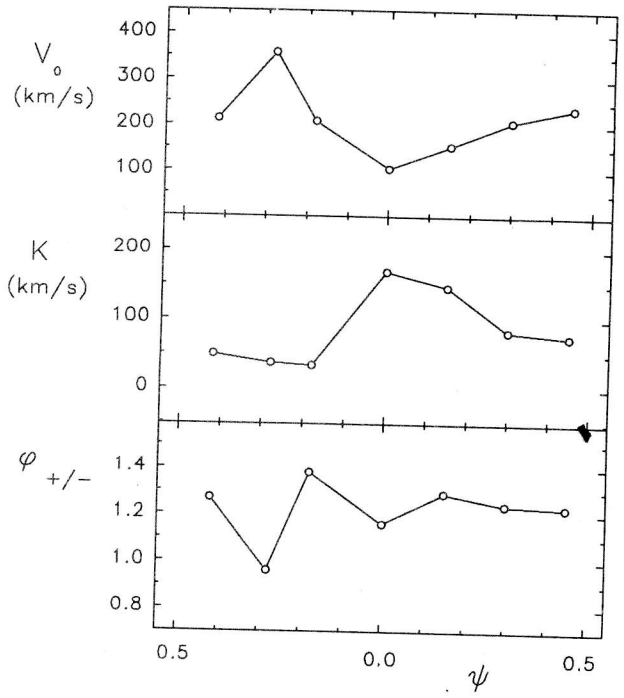

Figure 12: *The orbital curve parameters of the* Hβ *(p) line: mean radial velocity (top), half–amplitude (middle) and the superior conjunction phase (bottom) versus precession phase.*

of this line in the vicinity of $\psi = 0$ is the most free from the effects of the streams and the line absorption in the wind. At the same time the orbital curve phases demonstrate in addition that the most He II emission is formed in the accretion disk. At the same precession phases the orbital curve of He II has the least scatter, its half–amplitude is maximal and amounts to K $\approx$ 175 km/s. This value coresponds to a mass function $f(M) = M_0{}^3/(M_x + M_0)^2 \gtrsim 7.7\,M_\odot$ at the known orbital inclination angle i = 79°. The inequality means that, even being considered in a narrow interval of precession phases at $\psi \approx 0$, the He II line profile may contain a portion of emission which is formed in the stream. The mass function obtained proves the system SS 433 to be a massive binary. Assuming that the relativistic star has a mass typical of neutron stars $M_x = 1.4\,M_\odot$, the optical star mass appears then to be $M_0 = 10\,M_\odot$. The mass ratio of the stars in SS 433, which has been obtained from the solution of the light curves (Antokhina and Cherepashchuk, 1987), $q > 0.25$, and the most likely value of this is $q \approx 0.4$. Using the mass function found, one can obtain that $M_x > 3\,M_\odot$ or $M_x \gtrsim 6\,M_\odot$ as the most likely mass. This indicates that the relativistic component in the system SS 433 may be a black hole.

Table 3: *Parameters of orbital curves*

Line	ψ	V_0 km/s	K km/s	ϕ_{+-}	rms km/s	N
He II λ4686	0.90 – 0.10	78	176	0.06	61	21
	0.95 – 0.05	–4	180	0.06	66	11
	0.05 – 0.11	17	161	0.01	36	8
	0.11 – 0.20	119	102	0.32	100	12
	0.60 – 0.80	17	97	0.96	67	9
	0.80 – 0.95	–23	231	0.11	63	12
Hβ (p)	0.90 – 0.10	106	169	0.16	64	25
	0.10 – 0.20	156	147	0.29	69	18
	0.20 – 0.40	209	83	0.24	31	16
	0.20 – 0.67	216	67	0.25	36	41
	0.40 – 0.50	238	75	0.23	20	8
	0.50 – 0.67	214	49	0.27	38	17
	0.68 – 0.77	359	37	0.96	57	15
	0.77 – 0.90	209	33	0.38	61	11
Hβ (c g)	0.50 – 0.74	191	212	0.10	83	12
	0.74 – 0.76	324				10
	0.76 – 0.83	283	80	0.79	57	7
	0.83 – 0.90	206	159	0.20	62	8
	0.90 – 0.10	117	108	0.17	67	20
	0.10 – 0.30	89	172	0.31	82	18
He I λ5876	0.85 – 0.15	109	92	0.11	51	24
	0.15 – 0.30	–62	154	0.18	143	9
	0.50 – 0.70	216	226	0.96	84	5
	0.70 – 0.76	317	144	0.40	112	7
	0.76 – 0.85	122	106	0.36	46	8
He I λ6678	0.90 – 0.10	118	86	0.07	47	14
	0.10 – 0.20	93	101	0.19	63	9
	0.20 – 0.50	19	160	0.71	101	6
	0.50 – 0.72	81	257	0.10	61	13
	0.72 – 0.76	142				7
	0.76 – 0.90	251	161	0.04	75	13
He I λ7065	0.86 – 0.14	146	100	0.23	59	15
	0.14 – 0.50	311	79	0.95	50	6
	0.60 – 0.70	193	149	0.10	56	8
	0.70 – 0.86	257	128	0.14	63	16

3.4. The analysis of the absorption lines

In Figs. 7 – 10 the precession and orbital radial velocity curves of the absorption lines are shown. The zero point of the orbital curves is formal, the correct radial velocities are shown on the precession curves. Examination of the absorption line behaviour becomes quite important in interpretation of variability of emission lines and their relationship with the intensity and radial velocity of the absorptions that appear in the blue wing of the emission lines. Absorption distorts all emission line profiles. However, in the He II line the absorption in the blue wing can be revealed only from the behaviour of the emission line radial velocity, it is not directly seen in the spectra. The rest of the studied emission lines show narrow absorption lines. The Fe II λ5169 absorption is conspicuous, which, as a rule, is a purely absorption line in the spectrum of SS 433, without noticeable emission. This line is es-

pecially important for analysis as an example of the nondistorted absorption line. In the rest of the lines the orbital motion of emission must in turn change the absorption line radial velocity. When comparing the orbital behaviour of the Fe II line (Fig. 10 b) with that of the Hβ line (Fig. 7 b), it can be concluded that the orbital modulation of the lines is, apparently, not observed. The radial velocity of the Hβ absorption is actually variable with an amplitude of about 300 km/s, but even if the radial velocity of Fe II is variable, its variability amplitude is no higher than 100 km/s. On the other hand, when comparing the orbital variability of Hβ absorption with the behaviour of its associated emission at the same precession phases, 0.69–0.77 (Fig. 7 b and 2 b), one can see the phases of these curves to coincide completely. The emission line shows rather a noisy orbital curve of small amplitude in this precession phase interval. The Hβ emission line intensity is high and in this interval of ψ the absorption line is close to the emission peak, so a minor displacement of the emission line can appreciably distort the absorption line. From the data presented it can be concluded that the orbital variability of the absorption line radial velocities is due to the emission line variability.

In Fig. 10 a (bottom) we present the dependence of Fe II and He I absorption lines intensity on the precession phase from the data of Crampton and Hutchings (1981). It is seen from the figure that the absorption lines appear in the spectrum of SS 433 only at precession phases between 0.3 and 0.9. The vertical bars indicate the moments with an edge-on orientation of the accretion disk. The absorption line intensities show two symmetric maxima that delay behind the "disk edge-on" phases by a phase interval of 0.16 and 0.14 for the first and second maxima, respectively. For the value of delay derived from the absorption line intensities we can take the mean value $\Delta\psi(\mathrm{I_{abs}}) = 0.15$.

Our observations do not cover all precession phases in which the absorption lines occur, in particular, we can study the behaviour of these lines only at the time of the second maximum at precession phases 0.7–0.9. Because of the large amplitude of the radial velocity variation and the minor (or lacking) orbital variability, the precession curves before and after the correction for the orbital modulation are actually indistinguishable (Figs. 7 a – 10 a). At the moment the absorption lines appear in the spectrum ($\psi \approx 0.7$, "disk edge-on", the disk polar angle $\alpha \approx 90°$) they have an approximately zero velocity and a high intensity. This suggests that the gas outflowing from the disk is very dense in the disk plan and move at a low velocity. When the disk turns in the course of precession ($\psi > 0.7$, the line of sight is above the disk plan), the wind becomes less dense and accelerates. The absorption lines weaken and displace to velocities $-600 \div -1200$ km/s. The final radial velocity to which the line is displaced is different for different lines. It depends on the precession phase to which the absorption line is visible in the spectrum, i. e. on the line intensity or on the optical depth of the absorbent.

The line intensity is also dependent on the gas temperature in which the absorption is formed. In Fig. 10 a it is seen that the behaviour of the Fe II line (low ionization potential) is unusual. The limiting velocity of the absorption line is about 600 km/s. At $\psi \approx 0.95$, which is close to the maximal exposure of the accretion disk (maximal temperature of the source), the velocity of gas outflow in which this line is formed even decreases. The highest velocity absorptions are the most optically thick lines, they are Hβ and He I λ 5015 lines. The absorptions in these lines are also the most intensive. For these two lines we have only one observation at $\psi = 0.65$. The radial velocity of the lines at this phase is as high as at $\psi \approx 0.9$. Taking into account the above derived delay value ($\Delta\psi(\mathrm{I_{abs}}) = 0.15$), find that the phase of observation of the absorption lines, 0.65, is consistent with the moment of absorbing gas outflow, $\psi = 0.50$. At this moment the disk is exposed to a maximum, but from the its "rear" side ($\alpha = 81°$). It may well be supposed that the two surfaces of the accretion disk are symmetrical and the same (however, an azimuthal asymmetry is possible). That is why at $\psi = 0.65$ on the line of sight the gas is located outflowing from the other disk surface. All these data are in good agreement with the model we are discussing that the absorption lines are formed in matter outflowing from the accretion disk.

4. Interpretation and discussion of results

The absorption lines are formed in matter outflowing from the accretion disk. This follows from the behaviour of intensities and radial velocities of the absorption lines. The wind from the disk precesses as well as the disk itself. This type of precession is called slaved, it has first been proposed by Shakura (1972). For an absorption line to appear a sufficient optical depth in the outflowing matter must be accumulated on the line of sight. The appearance and intensification of the absorption lines twice over a precession cycle and their delay (with respect to the true "disk edge-on" phases) by $\Delta\psi(\mathrm{I_{abs}}) \approx 0.15$ is connected with the time needed for optical depth accumulation in the wind gas. From Figs. 7 a – 10 a it is seen that the absorption line radial velocity curves delay too. By measuring this delay as the difference between the "disk edge-on" phase ($\psi = 0.67$) and a radial velocity curve maximum, which corresponds to the moment of appearance of the absorption lines in the matter

blown out in the accretion disk plane, one can find for the lines Hβ and He I λ 5015 $\Delta\psi\,(H\beta) \approx 0.10$ and $\Delta\psi\,(\lambda\,5015) \approx 0.12$. The radial velocity curves of the other He I line and the line Fe II have no apparent maximum.

Using the known kinematic model of the SS 433 jets precession (Margon and Anderson, 1989), the obtained values of the radial velocity curve delays and also the curves themselves (Figs. 7 a and 9 a), we can find the wind velocity dependence V_W on the disk polar angle α. This relationship is displayed in Fig. 13, where the data on the Hβ and He I absorption lines are indicated by the open and filled circles, respectively. Based on the absorption lines, one can study the velocity (and a structure) of the wind from the supercritical accretion disk only at large polar angles since, according to the kinematic model, the accretion disk of SS 433 never gives a full face-on view, $\alpha \geq 59°$. In the figure is also shown the gas outflow velocity in the hot cocoons of He II around the relativistic jet bases (Fabrika et al., 1997 a). The interval of polar angles of the He II cocoons is not determined, it is supposed to be $10° \lesssim \alpha \lesssim 30°$. As the polar angle decreases, the gas outflow velocity rises sharply from 100 – 150 km/s at $\alpha = 90°$ to $V_W \approx 1300$ km/s at $\alpha \approx 60°$. In this range of α the wind velocity is well approximated by the relation $V_W = (8000 \pm 100\ \mathrm{km/s}) \cdot \cos^2\alpha + 150 \pm 10$ km/s. We can not study the wind at angles $20° \lesssim \alpha \lesssim 60°$, but in all likelihood the gas velocity in this interval of angles approaches 1500 km/s. Thus analysis of the absorption lines in the spectrum of SS 433 allows the wind structure and its velocity profile to be investigated.

The wind data are in excellent agreement with the model of supercritical accretion disks described first by Shakura and Syunyaev (1973). From our data it also follows that the outer parts of the disk of SS 433 are involved in precession motion. This implies that the angular momentum of a matter lost by the donor star precesses too. This suggest, in turn, that the model of a slaved accretion disk (Shakura, 1972) is valid for SS 433. According to this model the rotation axis of the optical star is not parallel to the orbital one, the star precesses under the action of force moment of the second component. The gas lost by the optical star forms an accretion disk whose precession motion traces that of the star. Both the wind and the jets formed in the disk are involved in the precession.

In the disk plane the most intensive gas loss may occur through the libration point L_2, this is due to the angular momentum loss when the disk is formed. An additional cause of angular momentum loss appears above the disk plane — the supercritical wind. The gas lost by the system through L_2 escapes from the system as a spiral out pattern (Fabrika, 1993). If we examine the wind density distribution along the line of sight, we will see that at small distances from the system, $r \lesssim 5 \cdot 10^{13}$ cm (which corresponds to a motion at a velocity of 100 – 150 km/s during several orbital cycles), the distribution of outflowing gas is inhomogeneous. The regions of enhanced density are modulated by the orbital period, they are separated by $(1 \div 1.5) \cdot 10^{13}$ cm. At greater distances from the system, the separation between the condensations and the amplitude of density variations must diminish, since the high-velocity gas ejected from the accretion disk later overtakes slower gas. At greater distances from the system the wind density along the line of sight is modulated with the precession period. The wind velocity at large distances from SS 433 may be supposed to be $V_T = 300 \div 400$ km/s, the separation between the gas condensations in this region is accordingly $\approx 5 \cdot 10^{14}$ cm. This conclusion proceeds from the interpretation of the behaviour of the Fe II λ 5169 absorption line radial velocities (Fig. 10 a). It is seen from the figure the velocity of the iron absorption line, as well as of hydrogen, rises as the disk opens up, but only up to -600 km/s. Such a wind velocity is reached at the polar angle $\alpha \approx 75°$. Higher above the disk plane the gas temperature rises so that the Fe II ion ceases to exist. However, the wind velocity measured from the Fe II line further decreases and at $\psi = 0.95$ (47 days after the "disk edge-on" phase, i. e. at larger distances) it is as low as $V_W = 300 \div 400$ km/s. We suppose that this is a terminal wind velocity resulting from interaction of fast and slow gas moving along the line of sight. The high-speed wind drags the slow wind issued in the accretion disk plane when overtaking the latter. At this place at a distance of $\approx 1.5 \cdot 10^{14}$ cm from the source conditions are likely to be created for the absorption Fe II line to be formed.

We have seen that the appearance of the absorption lines in the SS 433 spectrum is delayed with respect of the "disk edge-on" phase, which is due to the wind gas accumulation on the line of sight needed for line formation. The delay estimated from the behaviour of the Fe II and He I line intensities equals $\Delta\psi\,(I_{abs}) = 0.15$. That derived from radial velocities of the Hβ and He I λ 5015 absorption lines is $\Delta\psi\,(H\beta) \approx 0.10$ and $\Delta\psi\,(\lambda 5015) \approx 0.12$. Absorptions distort the emission line profiles. Because of that, the maximum of the emission line radial velocities falls not on the phase $\psi = 0.5$, as should be expected within the frame of a simple model the emission lines distortion due to absorptions, but is delayed by $\Delta\psi\,(\mathrm{em}) \approx 0.12 \pm 0.07$ over all the lines studied or by $\Delta\psi\,(H\beta) = 0.13$ for the line Hβ (p). All the delay estimates presented are very close to one another and independent in the sense that they have been measured from different lines and from different line parameters.

The distortion of the emission lines by the absorption lines must have an effect on the behaviour

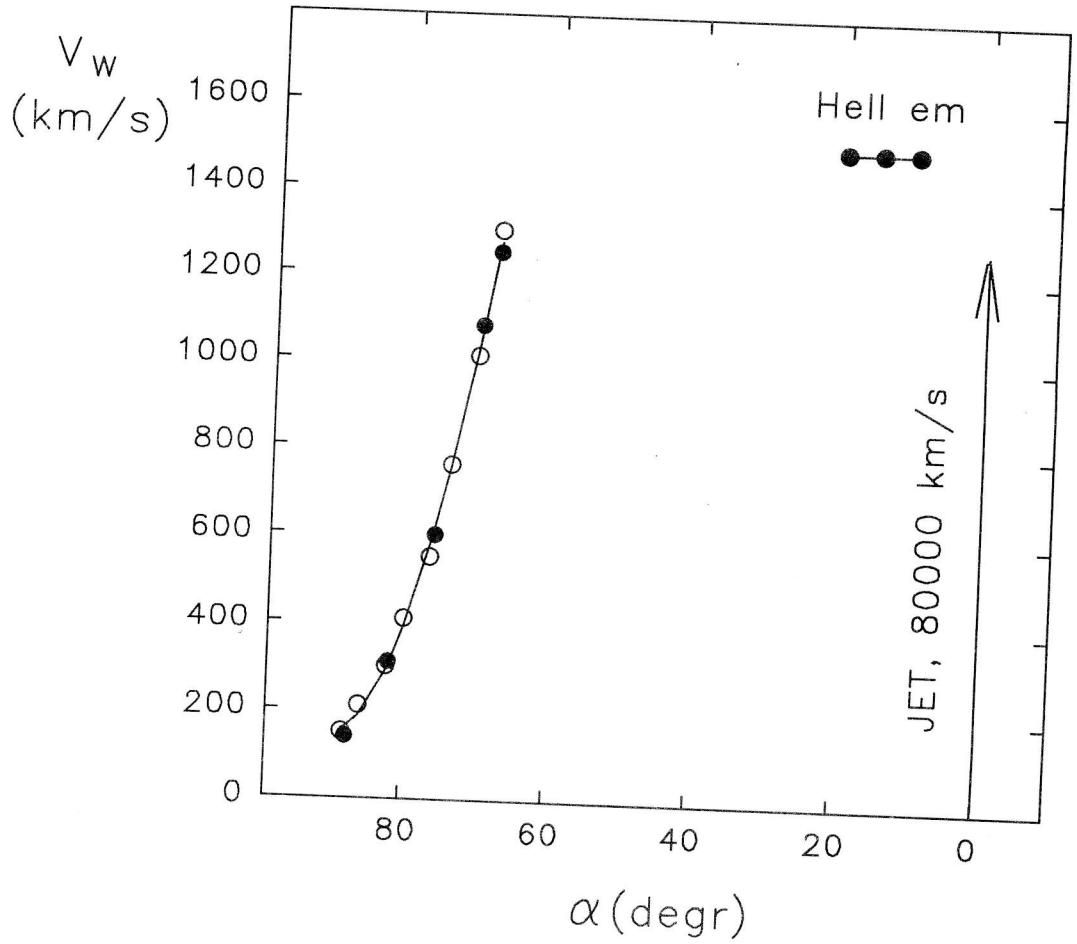

Figure 13: *The accretion disk wind velocity* V_W *versus the disk polar angle* α. *The data on the* $H\beta$ *and HeI* λ *5015 absorption lines are indicated by the open and filled circles, respectively. The data on HeII* λ *4686 were taken from Fabrika et al. (1997a).*

of the emission line intensities, which must decrease at the moment of maximum absorption in the line profile. In Fig 14 we present the emission line intensities in $10^{-10}\,\mathrm{erg\,cm^{-2}s^{-1}}$ corrected for interstellar absorption and averaged within the precession phase intervals for Hα (top), Hβ (middle) from the compilation of Asadullaev and Cherepashchuk (1986) and our individual measurements of Hβ (bottom). The systematic difference in Hβ line intensities from our and the published data is caused by the differences in the approximation of the SS 433 spectrum, which is strongly distorted by interstellar absorption (Fabrika et al., 1997b). In our data the triangles indicate the intensities obtained during SS 433 flares. The variation in the Hα intensity approximately follows a sine function, the intensity minimum delays behind $\psi = 0.5$ by $\Delta\psi(\mathrm{I_{H\alpha}}) = 0.19$. The similar value derived from the published data using the Hβ emission line is $\Delta\psi(\mathrm{I_{H\beta}}) = 0.13$, the data do not cover all precession phases, that is why the approximation may be inaccurate. Our data cover a still more narrow interval of precession phases, but they are not at variance with the compilative data. In particular, the maximum of intensities over all three sets of data are in the vicinity of $\psi = 0.1 \div 0.2$. Thus, the behaviour of Hα and Hβ line intensities is consistent with that of radial velocities of both the absorption and the emission lines and confirms the model of the SS 433 supercritical disk wind being discussed.

If the precession variability of the emission line radial velocities is basically (or completely) caused by the variability of the absorption components of the lines, then the modulation of the precession radial velocity curves could be also related with the absorption lines. The modulations found are most pronounced in the Hβ(p) line (Fig. 2b). In Fig. 15 we present the Hβ(p) emission line radial velocities versus the phase of the strongest of the found cycles, 23.228 days, in the precession phases interval 0.62 – 1.0. This curve is of high significance, its half–amplitude K = 115 km/s (rms = 60 km/s, n = 40). Below in the figure we exhibit the radial velocities of the corresponding absorption line convoluted with the same period. The absorption line does not show the periodicity with a

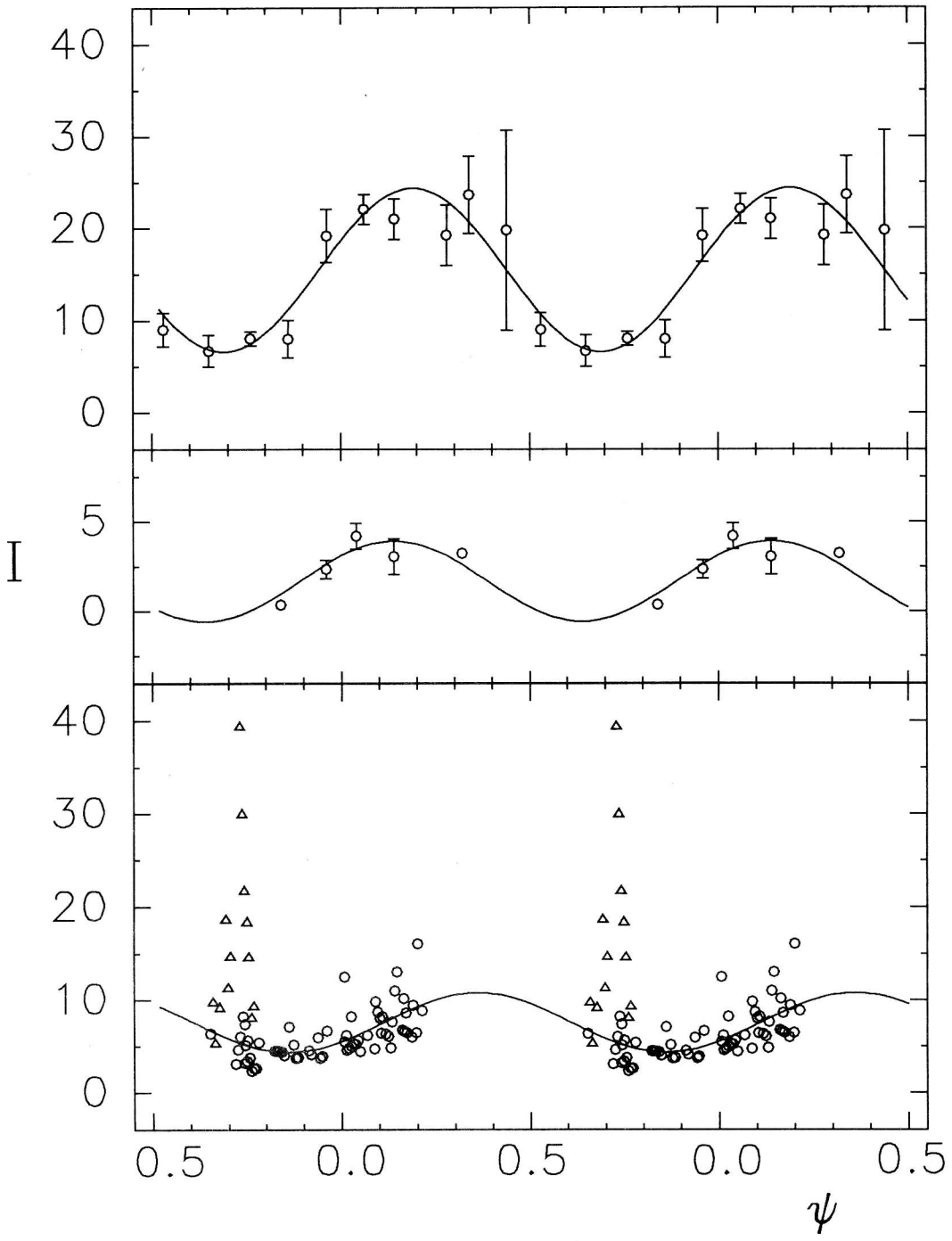

Figure 14: *Emission line intensities in* $10^{-10}\,\mathrm{erg\,cm^{-2}s^{-1}}$ *corrected for interstellar absorption for Hα (top), Hβ (middle) from the compilation of Asadullaev and Cherepashchuk (1986) and our individual measurements of Hβ (bottom).*

cycle of 23.2 days. This proves the variability of the radial velocities of emission lines with a period of 1/7 the precession period is not due to the variability of accompanying absorption lines.

The multiple period amplitudes change with precession phase. In particular, in Fig. 2b the radial velocity maximum at $\psi \approx 0.74$, which corresponds to the maximum in the variability with 23.2–days period, is especially pronounced. Compare the emission line behaviour with the behaviour of the absorption component of Hβ (Fig. 7 b). The maximum of the absorption line radial velocity falls on the same phase ($\psi \approx 0.76$), therefore the behaviour of the emission and absorption line is consistent here. However, if the

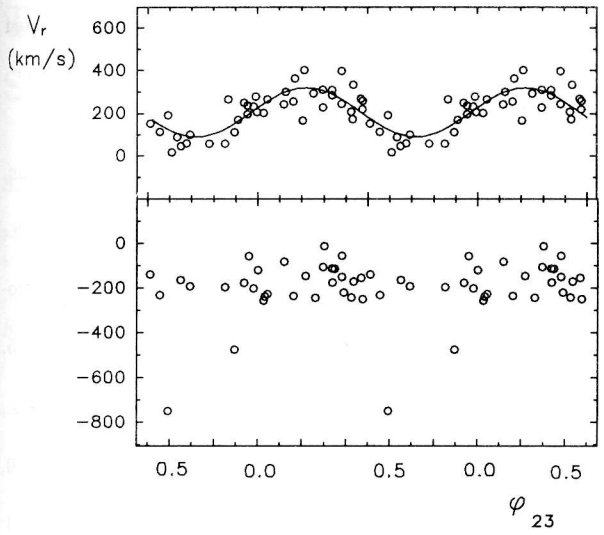

Figure 15: *The Hβ (p) emission (top) and absorption (bottom) line radial velocities versus the phase of the strongest cycle 23.228 days in the precession phase interval 0.62 – 1.0.*

absorption line radial velocity keeps falling down to $\psi \approx 0.95$, that of the emission line begins to rise (see Fig. 2 b), and at phases 0.85 – 0.90 it shows already a second peak in full accordance with the 23–days period. Thus, the variability of the emission line radial velocity with this period is not caused by the variability of the absorption line (which supports the conclusion made from Fig. 15). We may consider the coincidence of the two curves maxima at $\psi \approx 0.75$ (Figs. 2 b and 7 b) as an occasional.

We have seen the appearance of the cycle 1/7 of the precession period is not connected with the absorption lines which are formed in the wind (outside the binary system). That is why we believe the line variability with this period and, possibly, with other multiple periods originates in the accretion disk itself, i. e. it bears information on the structure of the disk. This variability may be caused by spiral density waves. Spiral shocks in accretion disks have repeatedly been considered in computer simulations (e.g. see Sawada et al., 1986). They arise when the gravitation potential differs from the axially symmetric one. The agent that disturbs potential in the accretion disks of binary systems is the second star (optical component). The number of spiral waves (multiplicity) is determined by the relation between the rotation velocity of matter and the sound velocity. Spiral shock waves in accretion disks are very effective in removal of angular momentum. Viscosity in an accretion disk determines the passing time of matter across the disk. Theoretical estimates of this time in accretion disks yield it to be of tens–hundred of days. In SS 433, apart of precession, a 6–days nutation of the jets is observed. The jets are formed in the inner region of the disk, that is why, for the nutation period be observable, one has to assume that the passing time is no more than 2 – 3 days or no more than a few revolutions of the disk. It is probable this "SS 433 problem" — the short passing time — is advantageously solved by shocks in the disk, which we observe in the emission line radial velocity variations.

Proceeding from the presented analysis we can not choose which of the multiple periods is fundamental. The spiral shock in SS 433 is likely to be 7–armed, which follows from the multiplicity of the strongest period found, 23.228 days. Depending on the precession phase, we observe the disk at different angles. The conditions for visibility of spiral shocks, i. e. the amplitude of the variations of the gas radial velocities, and, possibly, the recorded period of their propagation (multiplicity) must change with precession phase. The emission line radial velocity variability is best observable at the precession phases, when the disk is maximal exposed ($\psi = 0.8 \div 1.2$). At $\psi \approx 0.5$, when the disk is observed edge-on and even the reverse of the disk shows up, we see a 60–days period. The amplitude of the radial velocity variations with this period is markedly lower. It is probable that at this moment we observe a few 23–days cycle tandems at a phase shift because the reverse of the disk is observed.

5. Conclusions

Based on the spectral data obtained at the 6 m telescope and with involvement of data of other authors, we have revealed a precession modulation of the radial velocities of the strongest emission lines in the spectrum of SS 433. A variability of the orbital radial velocity curves of these lines has been detected and studied. The parameters of the orbital curves are essentially variable with precession phase. Phases have been isolated, when the contribution of the gas streams and absorption in the accretion disk wind distorts the line profiles the least. On this basis a correct mass function of SS 433 has been found, which indicates the system to be massive and its relativistic component may be a black hole. Absorption in the wind originating in the accretion disk is shown to be the main effect of the emission line variation with precession phase. Even the He II λ 4686 line with no absorption component observed in its profile is subject to this effect.

The radial velocities of the absorption lines are found to depend strongly on the precession phase and no dependence on the orbital phase is shown to exist. The structure of the gas outflow from the accretion disk has been found: in the disk plane the gas flows out at a low velocity, 100–150 km/s, probably through the libration point L_2. When approaching

the disk axis the gas density becomes lower and the wind velocity rises to $600 \div 1200$ km/s. The terminal velocity depends on the optical thickness of the line and on the ionization potential of the element. The optical depth sufficient for an absorption line to originate is accumulated at a distance of about $2 \cdot 10^{13}$ cm from the system. This causes the observed 20–days delay in appearance of absorption lines in the SS 433 spectrum and the same delay of the precession curves of the emission line radial velocities. The wind density distribution along the line of sight must be inhomogeneous. At small distances from the system, $r \lesssim 5 \cdot 10^{13}$ cm the regions of enhanced density are modulated by the orbital cycle, they are separated by $(1 \div 1.5) \cdot 10^{13}$ cm. At larger distances from the system the wind density is modulated with the precession period. It is assumed that at larger distances from SS 433 the wind flows out at a velocity $V_T = 300 \div 400$ km/s.

A number of new periods in the emission line radial velocity variations have been found, many of which are multiple of the precession one. The accuracy of strong multiple periods is comparable of that of the precession period determination. These periodicities can not be due to the variability of the absorption line components. These periods may be caused by spiral shocks in the accretion disk of SS 433. One can hope that a more detailed analysis of the emission line radial velocity variability will make it possible to reveal the cause of multiple periods and find the basic harmonics. The SS 433 precession provides a unique opportunity to study spiral shocks in accretion disks.

Acknowledgements. We thank I. M. Kopylov for helpful comments, V. D. Bychkov and G. G. Valyavin for help in the search for periods of radial velocity variations, T. A. Somova for processing of part of spectral data obtained in 1982. The work was supported by grant of the Programme "Astronomy" of RAS. The authors are grateful to ESO for support through grant of the C&EE Programme N A-02-021. L. V. Bychkova and A. A. Panferov wish to express gratitude to the American Astronomical Society for financial support. S. N. Fabrika was supported by grant of ISF.

References

Antokhina, E.A. and Cherepashchuk A.M., 1987, Astron. Zh., **64**, 562

Asadullaev S.S., Cherepashchuk A.M., 1986, Astron. Zh., **63**, 94

Crampton D., Cowley A.P., Hutchings J.B., 1980, Astrophys. J. (Lett.), **235**, 131

Crampton D., Hutchings J.B., 1981, Vistas in Astron., **25**, 13

Fabrika S.N., Bychkova L.V., 1990, Astron. Astrophys., **240**, L 5

Fabrika S.N., Kopylov I.M., Shkhagosheva Z.U., 1990, Preprint No. **61**, Nizhnij Arkhyz, SAO RAS

Fabrika S.N., 1993, Mon. Not. R. Astron. Soc., **262**, 241

Fabrika S.N., Panferov A.A., Bychkova L.V., Rakhimov V.Yu., 1997 a, Bull. Spec. Astrophys. Obs., **43**, (this issue), 95

Fabrika S.N., Goranskij V.P., Rakhimov V.Yu., Panferov A.A.,Bychkova L.V., Irsmambetova T.R., Shugarov S.A., Manirov T.K., Borisov G.V., 1997 b, Bull. Spec. Astrophys. Obs., **43**, (this issue), 109

Goranskij V.P., Fabrika S.N., Rakhimov V.Yu., Panferov A.A., Bychkova L.V., 1997, Astron. Zh., in press

Kopylov I.M., Bychkova L.V., Fabrika S.N., Kumajgorodskaya R.N., Somova T.A., 1989, Pis'ma Astron. Zh., **15**, 1092

Kopylov I.M., Kumajgorodskaya R.N., Somova T.A., 1985, Astron. Zh., **62**, 323

Kopylov I.M., Somov N.N., Somova T.A., 1986a, Astrofiz. Issled. (Izv. SAO), **22**, 77

Kopylov I.M., Kumajgorodskaya R.N., Somov N.N., Somova T.A., Fabrika S.N., 1986b, Astron. Zh., **63**, 690

Kopylov I.M., Kumajgorodskaya R.N., Somov N.N., Somova T.A., Fabrika S.N., 1987, Astron. Zh., **64**, 785

Margon B., Anderson S.F., 1989, Astrophys. J., **347**, 448

Sawada K., Matsuda T., Hachisu I., 1986, Mon. Not. R. Astron. Soc., **219**, 75

Shakura N.I., 1972, Astron. Zh., **49**, 921

Shakura N.I., Syunyaev R.A., 1973, Astron. Astrophys., **24**, 337